Journal of Soils and Sediments (2024) 24:2237–2247
https://doi.org/10.1007/s11368-024-03821-x

SOILS, SEC 1 • SOIL ORGANIC MATTER DYNAMICS AND NUTRIENT CYCLING • RESEARCH ARTICLE

Biochar effects on soil aggregation, phosphorus distribution, and colloidal phosphorus content in paddy soils: a comparative study

Jinju Wei[1] · Guobing Qin[1,2] · Qingyang Zeng[1] · Qi Luo[1] · Jianhua Ji[3] · Xiao Yan[1] · Jianfu Wu[1] · Zongqiang Wei[1]

Received: 20 December 2023 / Accepted: 13 May 2024 / Published online: 20 May 2024

Abstract

Purpose Soil colloids significantly influence the transfer of phosphorus (P) from agricultural lands to aquatic ecosystems. Nevertheless, the impact of soil amendments, such as biochar, on colloidal P release and mobilization is not fully understood. This study aimed to explore how biochar amendments affect the dynamics of soil colloidal P in paddy soils, particularly focusing on the interaction between soil aggregation and colloidal P mobilization.

Materials and methods We conducted a soil incubation experiment to investigate the effects of rape straw-derived biochar (SBC) and chicken manure-derived biochar (MBC) on soil aggregate stability, P distribution, and colloidal P content in paddy soils with different fertility levels. Soil aggregates were fractionated using wet sieving and sedimentation methods, whereas colloidal P was determined through ultracentrifugation.

Results and discussion Our findings demonstrated that both MBC and SBC addition increased soil aggregation by promoting the formation of larger aggregates (> 250 μm and 53–250 μm), while reducing the proportion of smaller soil aggregates (< 2 μm, 2–20 μm, and 20–53 μm). Biochar addition led to an increased allocation of P in soil aggregates of > 250 μm and 53–250 μm, with the observed rise in total P content primarily attributed to the inherent P within the added biochar. MBC exhibited a more pronounced impact on soil P dynamics than SBC. Despite enhanced soil aggregation, MBC addition substantially increased soil colloidal P and dissolved P, suggesting potential environmental risks associated with P loss. The elevated degree of P saturation resulting from MBC addition appeared to play a more critical role in regulating soil colloidal P release and mobilization.

Conclusion Our study highlights the importance of carefully considering the long-term application of P-enriched biochar in paddy soils, as this practice may lead to P loss even in the presence of increased soil aggregate stability.

Keywords Biochar · Soil aggregation · Soil colloids · Phosphorus · Paddy soil

1 Introduction

Soil colloids, which encompass particles with sizes in the range of 1 nm to 1 μm, exist in a suspended state in water, making them mobile entities within soil (Kretzschmar et al. 1999). Soil colloid-facilitated transfer of phosphorus (P) is a significant mechanism for P movement from agricultural land to aquatic ecosystems (Siemens et al. 2004; Ilg et al. 2005; Regelink et al. 2013; Liang et al. 2016; Gu et al. 2020). However, the release and mobilization of soil colloidal P in response to soil amendments, such as biochar, are not fully understood.

The practice of utilizing biochar, a product high in carbon generated through the pyrolysis of biomass (e.g., manure and crop residues), is becoming increasingly popular as a

Responsible editor: Zhaoliang Song

✉ Zongqiang Wei
zqwei85@mail.jxau.edu.cn

[1] School of Land Resource and Environment, Jiangxi Agricultural University, Nanchang 330045, China

[2] Hezhou Branch of Guangxi Academy of Agricultural Sciences, Hezhou 542813, China

[3] Soil and Fertilizer & Resources and Environment Institute, Jiangxi Academy of Agricultural Sciences, Nanchang 330200, China

soil amendment to improve soil fertility and promote carbon sequestration (Biederman and Harpole 2013; Schmidt et al. 2021). Previous studies have demonstrated that the application of biochar can directly and indirectly influence soil P mobility and availability. Direct effects can arise from certain biochars containing significant amounts of P, which may be released upon application (Jin et al. 2016; Jing et al. 2017). Indirectly, biochar addition can alter soil properties associated with P sorption, thereby affecting the mobility and availability of soil P (Zheng et al. 2020). However, these studies primarily focused on the effects of biochar on soil dissolved P, with limited information available on soil colloidal P.

Biochar amendment generally improves soil aggregation, although the extent of this effect may vary depending on the type of biochar, experimental conditions, and soil properties (Blanco-Canqui 2017; Islam et al. 2021). For example, biochar application has been found to promote soil aggregation by decreasing the proportion of soil aggregates with sizes < 0.25 mm in Acrisols (Li et al. 2017), Cambisols (Du et al. 2017), and Vertisols (Lu et al. 2014; Sun and Lu 2014). Enhanced soil aggregation due to biochar addition could potentially reduce the detachment of colloidal material, consequently decreasing soil colloidal P release and mobilization. However, it is important to note that further validation is required for this hypothesis, as conflicting results have been reported in studies regarding this issue. While some studies have suggested that biochar addition reduces colloidal P or particle-bound P losses by enhancing aggregate stability (Soinne et al. 2014; Wang et al. 2021), other studies have observed an increase in soil colloidal P with biochar addition (Kumari et al. 2014; Hosseini et al. 2019). To accurately assess the effects of biochar amendments on soil P status, it is crucial to understand the relationship between soil aggregation and soil colloidal P concentration.

Paddy soils, classified as Anthrosols and predominantly used for rice cultivation, are the largest anthropogenic wetlands globally (Kögel-Knabner et al. 2010; Liu et al. 2019). Due to long-term fertilizer and/or manure application, many paddy fields have experienced significant accumulation and loss of P, often exceeding seasonal plant nutrient absorption (Yan et al. 2013, 2017). In fact, colloidal P loss plays a significant role in P loss from paddy soils (Liang et al. 2016). Studying how soil aggregation affects the release and mobilization of colloidal P in these soils can provide valuable insights into the mechanisms underlying P loss.

In this study, we aimed to address the critical knowledge gap concerning how biochar amendments, with contrasting P contents (high P and low P), influence the dynamics of soil colloidal P in paddy soils, specifically, the interplay between soil aggregation and colloidal P mobilization. We hypothesized that (i) biochar addition will decrease soil colloidal P content, as the biochar addition can promote soil aggregation and thus reduce colloid materials release, and (ii) biochar with different P content will have different effect on soil colloidal P content. The findings of this research will contribute to the growing body of knowledge on the effects of biochar amendments on soil P dynamics and provide practical guidance for sustainable soil management in agricultural systems.

2 Materials and methods

Two paddy soils were collected from the plow layer (0–20 cm) of two rice paddy fields in a suburban area of Nanchang, China. Both soils are derived from Quaternary red clay and have been used for rice cultivation. However, they differ significantly in their P contents due to differences in agricultural practice and intensity. The paddy soil with a higher P content (hereafter Paddy_HP) has a long history of rice cultivation and has received a greater amount of P input from mineral and organic manure, whereas the paddy soil with a lower P content (hereafter Paddy_LP) has just recently been subjected to rice cultivation. Before use, the soil samples from each rice paddy field were mixed, air-dried, and ground to pass through a 2-mm sieve.

Rape straw and chicken manure were used to produce biochar. These materials were dried in an oven at 70 °C, ground and sieved using a 2-mm mesh. The feedstock (< 2 mm) was then wrapped in aluminum foil and pyrolyzed in a muffle furnace at 500 °C for 2 h. The muffle furnace was then turned off and the biochar was collected overnight after cooling. This process was used to produce two types of biochar: rape straw-derived biochar (SBC) and chicken manure-derived biochar (MBC). These represent cellulose/lignin biochar and manure biochar respectively, both of which are common types of biochar widely utilized in agricultural practices. The biochar was ground to < 1 mm prior to use.

2.1 Experimental design

The experimental design included 16 treatments: two types of biochar were added to two different soils at rates of 0, 2, 4, and 8% (w/w). These biochar addition rates were similar to previous studies (e.g., Zhai et al. 2015; Usman et al. 2016). Notably, the 8% biochar addition rate exceeds typical field application levels and was deliberately chosen to examine the effect of a wide range of biochar addition rates on soil aggregation. Each of these 16 treatments was replicated three times, yielding a total of 48 experimental units. For each replicate, 500 g of soil was mixed with a corresponding proportion of biochar in a plastic bottle. The soil-biochar mixtures were then randomly arranged and incubated at a constant temperature of 25 °C for 90 days. The bulk

densities were set at 1.02 g cm^{-3} for the Paddy_HP soil and 1.42 g cm^{-3} for the Paddy_LP soil, which is similar to the soil bulk density in the field. The soil moisture content was maintained at 70% of the maximum water holding capacity throughout the incubation period. Water loss was monitored weekly, and additional water was added as needed to maintain a constant soil moisture level. After incubation, the soil and biochar mixtures were sampled, air-dried, and ground to pass through a 2-mm sieve.

2.2 Soil aggregates fractionation and associated P determination

Soil aggregates fractionation was performed with an emphasis on the soil aggregates smaller than 0.053 mm, due to their potential close association with soil colloids (Jiang et al. 2015a, b). Five soil aggregate fractions were separated: > 250, 53–250, 20–53, 2–20, and < 2 µm. Ten grams of the incubated soil (< 2 mm) were added to 100 ml of deionized water and dispersed using a calibrated ultrasonic probe-type dispersion equipment (Xinyi-IID, Ningbo Xinyi, China) with an output energy of 44 J ml^{-1} suspension. The dispersed suspension was then successively wet sieved through sieves with apertures of 250 µm and 53 µm. The soil aggregates smaller than 53 µm (i.e., 20–53, and 2–20 µm) were obtained through repeated sedimentation and syphoning off the suspension at the appropriate depths, calculated according to Stoke's law with an assumed particle density of 2.65 g cm^{-3} (Jiang et al. 2015b; Wang et al. 2016). Each isolated fraction was subsequently oven-dried at 50 °C, weighed, and its mass proportion was calculated as a fraction of the total dry mass of the bulk soil. The mass proportion of aggregates < 2 µm was determined by subtracting the masses of the other soil aggregate fractions from the mass of the bulk soil. We did not exclude the sand fraction when calculating the proportions of soil aggregates (> 250 µm and 53–250 µm) due to the difficulty in removing biochar particles, especially at higher biochar addition rates (e.g., 8%).

The total P content of each soil aggregate fraction except for the < 2 µm fraction was determined using the molybdenum blue method (Murphy and Riley 1962), after digestion with perchloric acid (Kuo 1996). The total P of the < 2 µm fraction was not determined, as the difference in total P between the bulk soil and other soil aggregate fractions also includes water-dissolved P.

In the soil aggregates of > 250 µm and 53–250 µm, there was a considerable amount of biochar (Fig. S1). To delineate the impact of biochar on the mass proportion and total P content within these aggregates, the contribution of biochar was estimated. Based on the carbon differential between amended and non-amended treatments (assuming the carbon solely originated from biochar), and considering the carbon and P content of the biochar, the mass of biochar and the total P contributed by biochar in the > 250 µm and 53–250 µm aggregates were calculated.

2.3 Soil colloidal P

Water dispersible soil colloidal P was determined to assess soil colloidal P release and mobilization. In brief, 5 g of incubated soil (< 2 mm) was dispersed using ultrasonication in 40 ml of deionized water, as previously described. After dispersion, the extract was centrifuged at 3000 × *g* for 10 min and filtered through 1 µm membrane. An aliquot of the sample that had been filtered through 1 µm was then ultracentrifuged at 300 000 × *g* for 1 h to remove colloids (CP100NX, Himac, Japan) (Ilg et al. 2005). The total P concentrations in non-ultracentrifuged (total P) and ultracentrifuged (dissolved P) samples were measured colorimetrically using the malachite green method after acid-persulfate digestion (Ohno and Zibilske 1991). The concentrations of colloidal P were calculated by subtracting the P concentrations in ultracentrifuged samples from those in non-ultracentrifuged samples.

The release and mobilization of soil colloidal P are known to be influenced by soil P sorption characteristics, particularly the degree of P saturation (DPS) (Siemens et al. 2004; Ilg et al. 2005; Fresne et al. 2021; Khan et al. 2022). Therefore, we further determined the DPS of the incubated soil by calculating the ratio of oxalate extractable P (P_{ox}) to the combined oxalate extractable aluminum (Al_{ox}) and iron (F_{eox}) contents, i.e., $P_{ox}/0.5(Al_{ox}+Fe_{ox})$ (Dou et al. 2009). The Al_{ox}, Fe_{ox}, and P_{ox} contents of the incubated soil were determined by shaking a 1:40 (w:v) soil:extracting solution of ammonium oxalate (pH 3.0) for 2 h, and then quantified by inductively coupled plasma optical emission spectroscopy (ICP-OES) using an Optima 8000 instrument (PerkinElmer, USA) (Courchesne and Turmel 2008).

2.4 Analysis of basic properties of soil and biochar

The particle size distribution of the soil was determined using the pipette method (Kroetsch and Wang 2008), and the pH was measured using a pH meter (FiveEasy, Mettler Toledo, China) in deionized water at a ratio of 1:2.5 (w:v). Soil total carbon and nitrogen were measured using an elemental analyzer (Vario MACRO Cube, Elementar, Germany), and total P was determined using colorimetry after perchloric acid digestion (Kuo 1996).

The particle size distribution of the biochar was determined using a laser diffraction instrument (Malvern Mastersizer 2000, Malvern, UK), and the pH of the two types of biochar was measured using a pH meter (FiveEasy, Mettler Toledo, China) in deionized water at a ratio of 1:30 (w:v) (Qin et al. 2022). Total concentrations of P, sodium (Na), potassium (K), calcium (Ca), magnesium (Mg), Fe, and Al of the biochar were measured by igniting the biochar in a muffle

furnace for 2 h at 550 °C and extracting it with 0.1 M HCl for 16 h. The resulting supernatants were analyzed for P, Al, Fe, Ca, and Mg using ICP-OES, and Na and K using a flame photometer. Total carbon and nitrogen of the biochar were also determined using an elemental analyzer (Vario MACRO Cube, Elementar, Germany). The specific surface area and pore volume of the biochar were determined using nitrogen gas adsorption (TriStar II 3020, Micromeritics, USA).

To determine the P forms in the biochar, solution ^{31}P nuclear magnetic resonance (NMR) spectroscopy was used. At a temperature of 25 °C and for a period of 16 h, the biochar was subjected to extraction with a solution containing 0.25 M NaOH and 0.05 M Na_2EDTA solution (1:10, w/v). Subsequently, the extract was filtered, frozen at −80 °C, and lyophilized to prepare for ^{31}P NMR analysis. After redissolving the lyophilized extract with 0.6 ml of D_2O and 0.1 ml of 10 M NaOH, the mixture was placed in a 5-mm NMR tube and subjected to analysis. The ^{31}P NMR spectra were obtained using a Bruker Avance III 400 spectrometer (Bruker, Germany) running at 162 MHz. The device parameters included an 8.00 µs pulse width (P1), a 65536 time domain (td), a 0.5 s acquisition time (aq), and a 2 s recycle delay (d1). The peak assignments of the biochar extracts were derived from Turner et al. (2003), with the orthophosphate peak in each sample adjusted to 6 ppm.

2.5 Statistical analyses

Statistical analyses were conducted using the R statistical program (version 3.6.1) (R Core Team 2019). A three-way analysis of variance (ANOVA) was performed to examine the effect of soil type (Paddy_HP, Paddy_LP), biochar type (MBC, SBC), and biochar addition rate (0, 2%, 4%, 8%) on the mass distribution of soil aggregates and the P content within them. Furthermore, a one-way ANOVA was conducted to identify significant differences among different levels of biochar addition for each soil and biochar type. The data were checked for normality and homogeneity, and log-transformations were utilized if necessary. Multiple comparisons between means were performed using Tukey's honest significant difference (HSD) test to identify significant differences between various biochar addition levels using the agricolae package (de Mendiburu 2014).

3 Results

3.1 Soil and biochar characterization

The two paddy soils had similar particle size distributions but distinct differences in other soil properties associated with soil fertility, such as carbon, nitrogen, total P, and extractable P, due to different agricultural management practices (Table 1). Compared with SBC, MBC contained significantly higher levels of total P and $NaHCO_3$ extractable P. Solution ^{31}P NMR further revealed that the P present in the NaOH-EDTA extracts from SBC and MBC biochars was exclusively inorganic P, with SBC predominantly containing orthophosphate, whereas MBC mainly contained orthophosphate and pyrophosphate (Fig. 1). The specific surface areas of MBC and SBC were 2.55 $m^2\ g^{-1}$ and 3.20 $m^2\ g^{-1}$, respectively, while their pore volumes were 0.013 $cm^3\ g^{-1}$ and 0.009 $cm^3\ g^{-1}$, respectively. Moreover, the volume mean diameter was 805 µm for MBC and 319 µm for SBC. The mass fractions of biochar components within the size range > 53 µm were 88.24% and 87.59% for MBC and SBC, respectively (Table 1). This suggests that the biochar is likely to reside mainly within soil aggregates of 53 – 250 µm and > 250 µm.

3.2 Soil aggregate distribution

Generally, the impact of biochar type on soil aggregate distribution was relatively weaker compared to soil type and biochar addition rate (Table 2). In fact, both types

Table 1 Basic properties of the soil and biochar

Parameter	Paddy_HP	Paddy_LP	MBC	SBC
Sand (0.05 – 2 mm), g kg^{-1}	246	279	–	–
Silt (0.002 – 0.05 mm), g kg^{-1}	515	500	–	–
Clay (< 0.002 mm), g kg^{-1}	239	221	–	–
pH	5.14	6.40	10.32	10.19
Total C, g kg^{-1}	19.92	3.83	387	530
Total N, g kg^{-1}	2.50	0.63	45.20	13.95
Total P, g kg^{-1}	1.36	0.41	28.79	4.94
$NaHCO_3$ extractable P, mg kg^{-1}	57.49	7.63	1138	381
Total Na, g kg^{-1}	–	–	0.16	0.06
Total K, g kg^{-1}	–	–	49.19	63.75
Total Ca, g kg^{-1}	–	–	58.26	77.08
Total Mg, g kg^{-1}	–	–	16.50	5.22
Total Fe, g kg^{-1}	–	–	4.51	1.86
Total Al, g kg^{-1}	–	–	1.76	0.82
Volume mean diameter, µm	–	–	805	319
Surface area, $m^2\ g^{-1}$	–	–	2.55	3.20
Pore volume, $cm^3\ g^{-1}$	–	–	0.013	0.009
Mass fraction (0.25 – 1 mm), %	–	–	60.18	53.90
Mass fraction (0.053 – 0.25 mm), %	–	–	28.06	33.69
Mass fraction (< 0.053 mm), %	–	–	11.76	12.41

The mass fractions of the biochar components within the size ranges of 0.25 – 1 mm, 0.053 – 0.25 mm, and < 0.053 mm were determined by sieving

MBC represents chicken manure-derived biochar, *SBC* represents rape straw-derived biochar

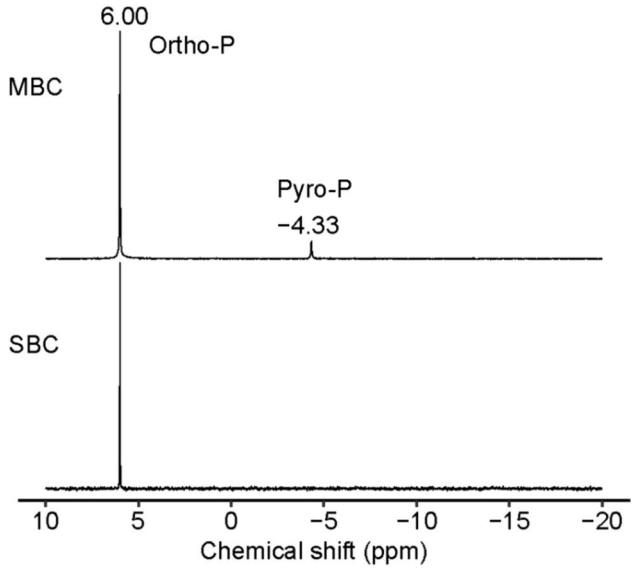

Fig. 1 Solution ^{31}P NMR spectra of chicken manure-derived biochar (MBC) and rape straw-derived biochar (SBC). Orth-P, orthophosphate; Pyro-P, pyrophosphate

of biochar had similar effects on the distribution of soil aggregates. Adding MBC or SBC to paddy soils resulted in an increase in the proportion of soil aggregates with sizes > 250 µm and 53–250 µm, respectively (Fig. 2). This increase in larger soil aggregates was accompanied by a decrease in the mass proportion of aggregates in the 20–53 µm, 2–20 µm, and < 2 µm size classes, suggesting that the increase in larger aggregates came at the expense of smaller ones.

3.3 P allocation in soil aggregates

The addition of both MBC and SBC biochars to soils led to an increase in the P content in soil aggregates (Fig. 3, Table 2). This effect was particularly pronounced when MBC was added, with the greatest increase observed in the > 250 µm and 53–250 µm size classes. For instance, in Paddy_LP soil, MBC biochar addition at 8% led to a 16-fold and 18-fold increase in total P content in the > 250 µm and 53–250 µm size classes, respectively, compared to the control treatment without biochar. However, it is important to note that the total P detected in the soil aggregates of > 250 µm and 53–250 µm was nearly entirely attributed to the MBC biochar (Fig. 4), as a considerable amount of biochar was present in these soil aggregates (Fig. S1). The notable increase in total P content in soil aggregates of > 250 µm and 53–250 µm subsequently led to a clear increase in their contribution to soil total P. In contrast, although the total P content in the 20–53 µm and 2–20 µm soil aggregates also increased due to biochar addition, their contribution to soil total P decreased (Fig. 5).

3.4 Soil colloidal P and dissolved P

Both MBC and SBC biochars led to an increase in the concentrations of water dispersible soil colloidal P and dissolved P, with MBC showing a more pronounced effect (Fig. 6). Specifically, MBC induced a significant increase in the dissolved P fraction of the total dispersible P, whereas its impact on the colloidal P fraction was relatively modest.

In contrast, the effect of SBC on the increase in water dispersible soil colloidal P and dissolved P was markedly lower. Particularly, in the Paddy_LP soil with SBC addition, the levels

Table 2 ANOVA results testing the effect of soil type (Paddy_HP, Paddy_LP), biochar type (chicken manure-derived biochar, rape straw-derived biochar), and biochar addition rate (0, 2%, 4%, 8%) on the mass distribution of soil aggregates and the P content within them

	> 250 µm	53–250 µm	20–53 µm	2–20 µm	< 2 µm
	Mass proportion of aggregate (g g^{-1} soil)				
Soil	< 0.001	< 0.001	< 0.001	< 0.001	< 0.001
Biochar	0.44	0.007	0.66	0.11	< 0.001
Rate	< 0.001	< 0.001	< 0.001	< 0.001	< 0.001
Soil×Biochar	0.04	< 0.001	0.49	< 0.001	< 0.001
Soil×Rate	0.52	< 0.001	0.009	0.64	0.04
Biochar×Rate	0.20	0.72	0.39	0.72	0.03
Soil×Biochar×Rate	0.84	0.08	0.25	0.33	0.25
	P content of aggregate (mg kg^{-1} aggregate)				
Soil	< 0.001	< 0.001	< 0.001	< 0.001	–
Biochar	< 0.001	< 0.001	< 0.001	< 0.001	–
Rate	< 0.001	< 0.001	< 0.001	< 0.001	–
Soil×Biochar	0.27	< 0.001	< 0.001	0.60	–
Soil×Rate	0.003	< 0.001	< 0.001	< 0.001	–
Biochar×Rate	< 0.001	< 0.001	< 0.001	< 0.001	–
Soil×Biochar×Rate	0.02	< 0.001	< 0.001	0.001	–

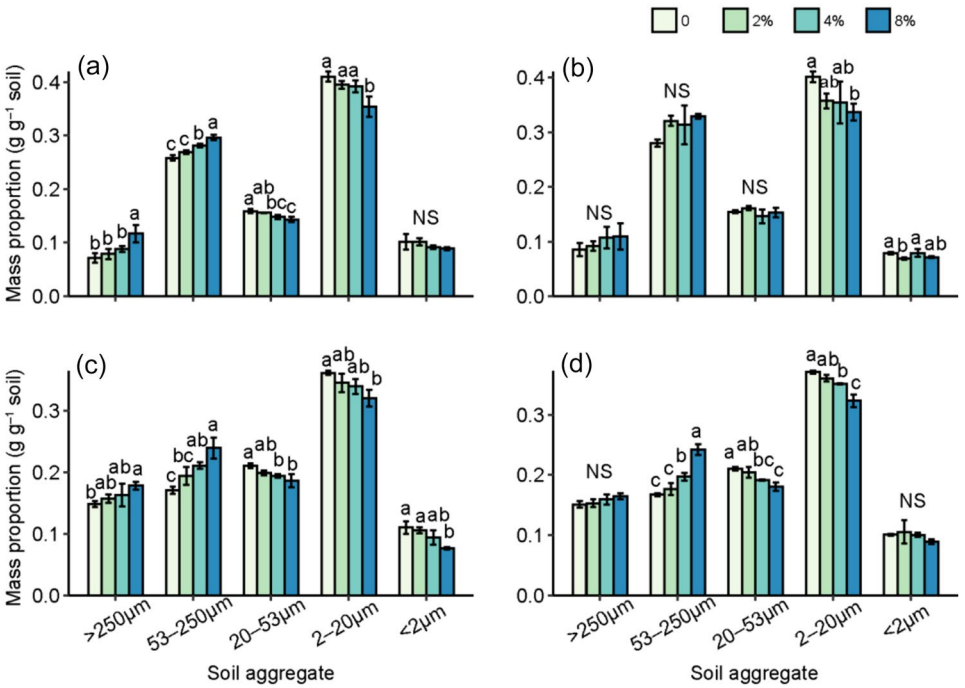

Fig. 2 Effects of adding chicken manure-derived biochar (MBC) and rape straw-derived biochar (SBC) at various addition rates (0, 2%, 4%, and 8%) on the mass proportion of soil aggregates in Paddy_HP and Paddy_LP soils. Panels **a** and **b** show the effects of MBC and SBC on the mass proportion of soil aggregates for Paddy_HP, while panels **c** and **d** show the effects of MBC and SBC on the mass proportion of soil aggregates for Paddy_LP. Values are means ± 1 standard deviation. Different letters indicate significant differences among the four biochar addition rates for each type of biochar in each soil. The mass proportion of aggregates < 2 μm was calculated by subtracting the mass of the bulk soil and the other soil aggregate fractions. NS, not significant

of colloidal P were too low to be accurately measured. In the case of Paddy_HP soil with SBC addition, the highest concentrations of soil colloidal P and dissolved P were found with an 8% adding rate. Nevertheless, these values were still lower compared to the respective parameters under MBC biochar addition (colloidal P: 0.99 mg kg^{-1} vs. 1.20 mg kg^{-1}; dissolved P: 1.14 mg kg^{-1} vs. 27.7 mg kg^{-1}). Regardless of soil and biochar types, there was a positive correlation between water dispersible soil colloidal P and both DPS and soil dissolved P (Fig. 7).

4 Discussion

4.1 Biochar effect on soil aggregation

The addition of both MBC and SBC resulted in an increase in the proportion of soil aggregates 53–250 μm and > 250 μm. This aligns with findings from both laboratory soil incubation studies (Lu et al. 2014; Soinne et al. 2014; Sun and Lu 2014) and field studies (Du

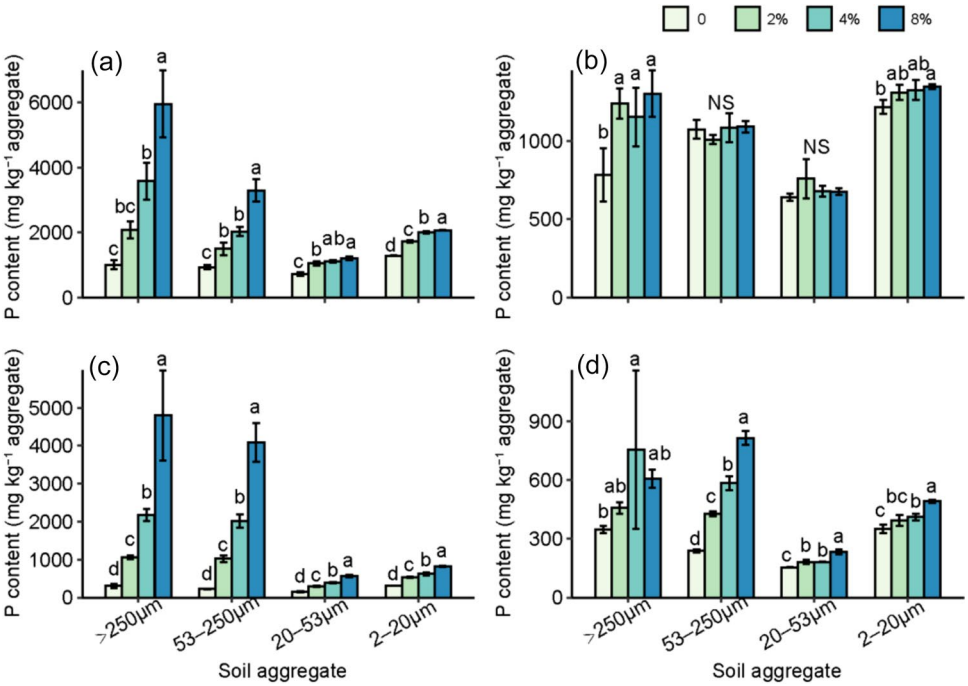

Fig. 3 Variations in P content across different soil aggregate size fractions in Paddy_HP and Paddy_LP soils, following the addition of chicken manure-derived biochar (MBC) and rape straw-derived biochar (SBC) at different addition rates (0, 2%, 4%, and 8%). Panels **a** and **b** show the effects of MBC and SBC on P content within soil aggregates for Paddy_HP, while panels **c** and **d** show the effects of MBC and SBC on P content within soil aggregates for Paddy_LP. Values are means ± 1 standard deviation. Different letters indicate significant differences among the four biochar addition rates for each type of biochar in each soil. NS, not significant

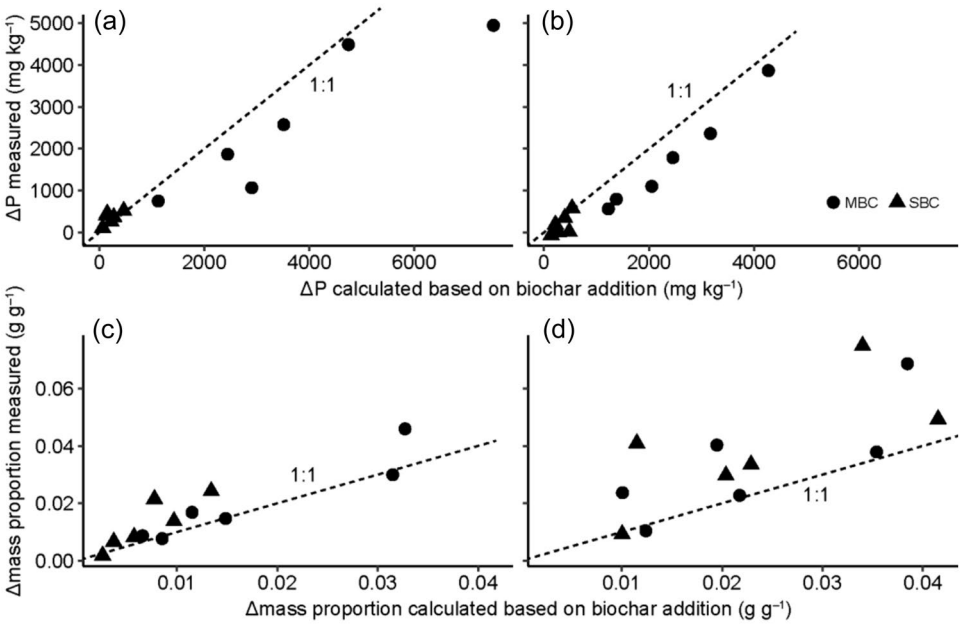

Fig. 4 Changes in P content (ΔP) measured in soil aggregates > 250 µm (**a**) and 53–250 µm (**b**), and changes in mass proportion (Δmass proportion) of soil aggregates > 250 µm (**c**) and 53–250 µm (**d**) due to the addition of chicken manure-derived biochar (MBC) or rape straw-derived biochar (SBC) compared to calculated values based on biochar addition. The data points represent the arithmetic mean of three replicates. The dashed line represents the 1:1 line, where measured and calculated values are equal

et al. 2017; Li et al. 2017; Situ et al. 2022), which have reported an increase in the proportion of macro-aggregates (e.g., > 250 µm) and a corresponding decrease in smaller aggregate fractions (e.g., < 250 µm and < 53 µm) upon the addition of biochar. Although a significant amount of biochar was found within the 53–250 µm and > 250 µm aggregates, the observed mass increase in these aggregates generally exceeded the mass of biochar added (Fig. 4), suggesting that biochar contributes to enhanced soil aggregation beyond just its physical addition. The carbon introduced by the biochar may act as a binding agent to glue the soil aggregates with small sizes (e.g., < 53 µm) together into macro-aggregates. In response to biochar addition, soil organic matter concentration and soil aggregate stability often exhibit a strong correlation (Blanco-Canqui 2017; Islam et al. 2021; Situ et al. 2022), indicating that carbon introduced by biochar can enhance soil

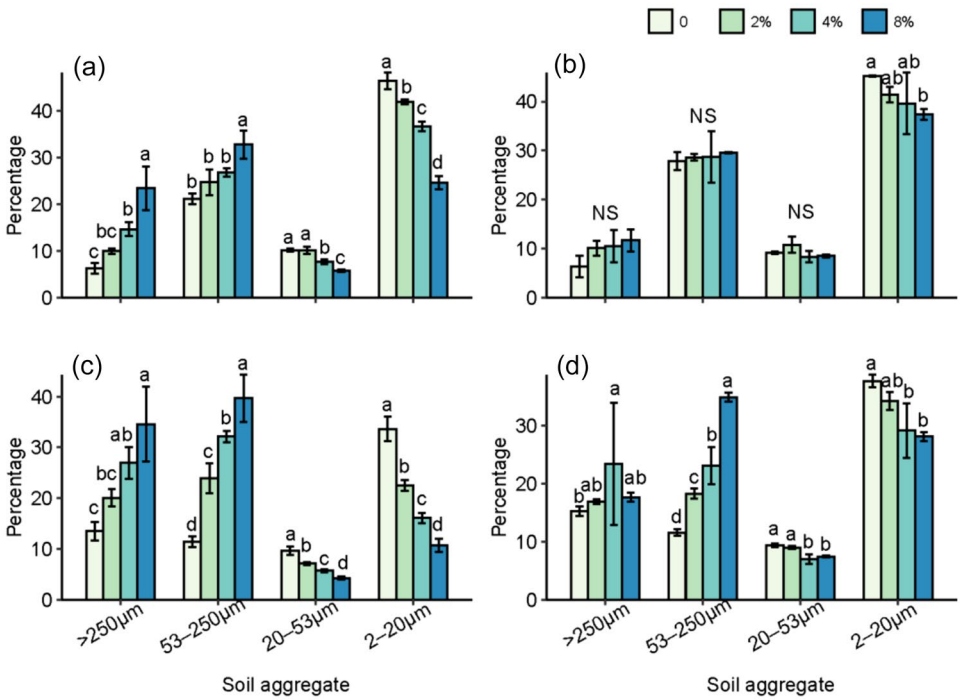

Fig. 5 Percentage of P in soil aggregates relative to soil total P for Paddy_HP and Paddy_LP soils subjected to addition of chicken manure-derived biochar (MBC) and rape straw-derived biochar (SBC) at different addition rates (0, 2%, 4%, and 8%). Panels **a** and **b** show the effects of MBC and SBC on the percentage of P in soil aggregates for Paddy_HP, while panels **c** and **d** show the effects of MBC and SBC on the percentage of P in soil aggregates for Paddy_LP. Values are means ± 1 standard deviation. Different letters indicate significant differences among the four biochar addition rates for each type of biochar in each soil. NS, not significant

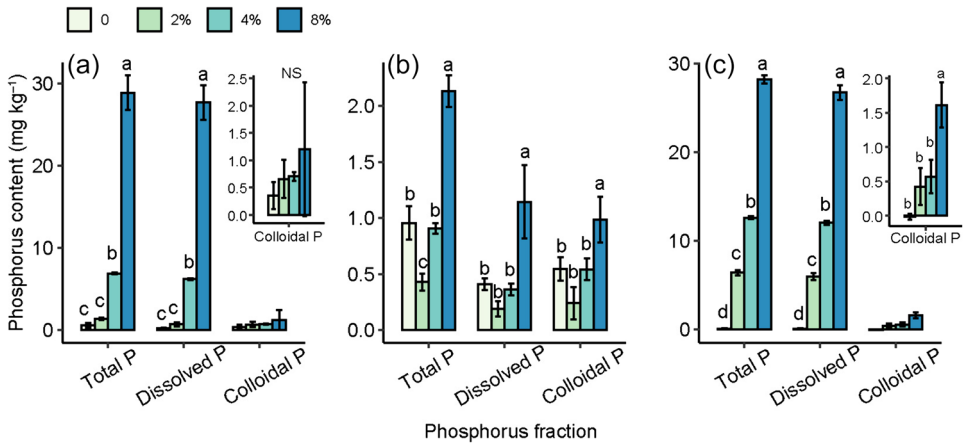

Fig. 6 Concentrations of total, dissolved, and colloidal P in water-dispersed soil samples from Paddy_HP and Paddy_LP soils treated with chicken manure-derived biochar (MBC) and rape straw-derived biochar (SBC) at various addition rates (0, 2%, 4%, and 8%). Panels **a** and **b** show the effects of MBC and SBC biochar addition on Paddy_HP, while panel **c** shows the effect of MBC biochar addition on Paddy_LP. Values are means ± 1 standard deviation. Different letters indicate significant differences among the four biochar addition rates for each type of biochar in each soil. Note that data for Paddy_LP soil with SBC addition is not shown due to low levels of soil colloidal P that could not be accurately measured. NS, not significant

aggregation and stability. Furthermore, both MBC and SBC biochars contained considerable amounts of minerals and exchangeable cations, which may further promote aggregate formation through polyvalent cationic bridging (e.g., Ca^{2+} and Mg^{2+}) with soil organic matter and soil colloidal minerals (Zheng et al. 2018; Sun et al. 2021). This is due to the typically negative charge of soil colloids and soil organic matter, such as humic substances. It is worth noting that MBC and SBC also contained significant K content. Although previous study reported that the K^+ may contribute to the dispersion of soil aggregates (Pituello et al. 2018), our study found higher biochar additions did not increase aggregate dispersion.

4.2 Biochar effect on the P distribution in soil aggregates

Biochar addition resulted in a higher allocation of P within soil aggregates of > 250 µm and 53–250 µm size classes. Although P concentration (expressed as mg kg^{-1} aggregate) increased in the 20–53 µm and 2–20 µm soil aggregate fractions, their contribution to soil total P exhibited a decline. The decrease in the proportion of total P in the soil aggregates of 20–53 µm and 2–20 µm to the soil total P could be ascribed to a reduction in the mass proportion of these two soil aggregate size classes (Fig. 2). Additionally, the biochar-induced increase in total P in soil aggregates larger than 53 µm diluted the proportion of P within smaller aggregates of 20–53 µm and 2–20 µm.

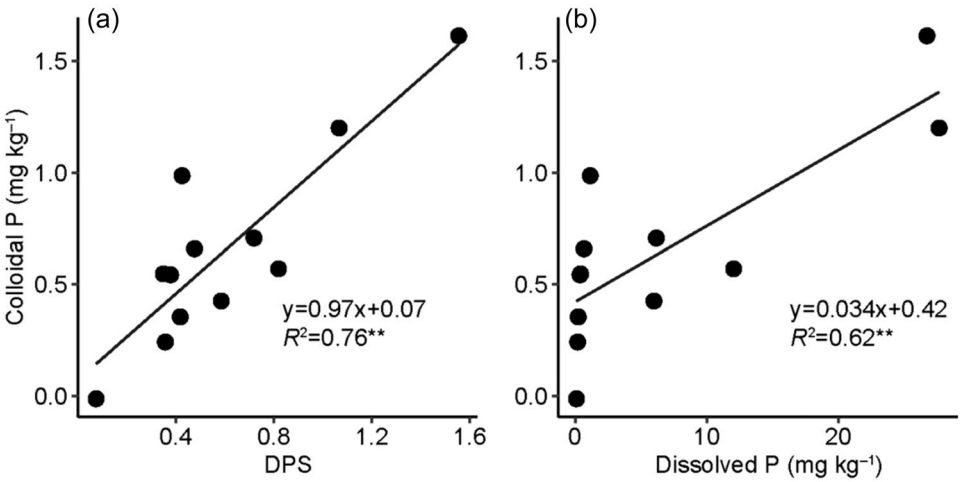

Fig. 7 Relationship between water dispersible soil colloidal P and degree of P saturation (DPS) (**a**) and soil dissolved P (**b**). The data points represent the arithmetic mean of three replicates. Note that the data for Paddy_LP soil with SBC addition is not included, as the soil colloidal P levels were too low to be accurately measured

This observation is consistent with the findings of a five-year field trial by Cao et al. (2021), who reported that biochar addition increased the accumulation of P in soil aggregates of 250–2000 µm. Similarly, Sachdeva et al. (2019) suggested that biochar addition could enhance P retention in macro-aggregates. The increase in total P in the > 250 µm and 53–250 µm soil aggregate size classes, as observed in our study, was primarily attributed to the biochar itself, which was primarily located within these aggregate fractions. We discovered that the P present in both SBC and MBC was predominantly inorganic P (both orthophosphate and pyrophosphate) (Fig. 1), which is consistent with previous studies (Jin et al. 2016; Xu et al. 2016). Therefore, we propose that inorganic P from biochar within > 250 µm and 53–250 µm soil aggregates size classes may not be stable in the long term due to the weaker retention capacity of soil minerals in these fractions (> 53 µm) compared to silt and clay fractions. Instead, the inorganic P in biochar is likely to be released through dissolution processes and adsorbed by silt and clay fractions (Wang et al. 2015; Garland et al. 2018). Consequently, the observed increase in P concentration within the 20–53 µm and 2–20 µm soil aggregate fractions could be due to the re-adsorption of P released from biochar, as biochar itself was absent in these fractions owing to its size. In this context, it is recommended to pay attention to the potential loss of P carried by small particles (e.g., 2–20 µm) via runoff or erosion from paddy fields, particularly when biochar with high P content is applied.

4.3 Biochar effect on soil colloidal P and dissolved P

Our initial hypothesis proposed that the concentration of soil colloidal P would decrease due to the organic carbon provided by biochar binding with colloids, which in turn would restrict the release of soil colloids (Wang et al. 2021). However, contrary to our hypothesis, the addition of MBC to paddy soils resulted in an increase in the concentration of colloidal P despite the enhancement in soil aggregation. This finding aligns with the observations of Hosseini et al. (2019), who also reported an increase in soil colloidal P following the application of sheep manure-derived biochar.

We discovered a significant and positive correlation between soil colloidal P concentration and the DPS as well as dissolved P concentration, particularly in the MBC treatment. The increase in soil colloidal P concentration might be attributed to the increase in P concentration within individual colloidal particles or the additional release of colloids from the soil. Upon addition to the soil, MBC can release a substantial amount of P, markedly elevating the concentration of dissolved P. This dissolved P could subsequently be re-adsorbed by soil colloids, thereby increasing the P concentration of individual soil colloidal particles. The abundant P input through MBC addition also elevated the DPS of the paddy soils (Fig. S2). The increased sorption of phosphates may result in a reduction in the positively charged surface potential of iron oxides and clay minerals, resulting in the dispersion of soil colloidal particles (Siemens et al. 2004; Ilg et al. 2005). Additionally, biochar additions can increase dissolved organic carbon levels in soil, potentially acting as a carrier for soil colloids. Hosseini et al. (2019) have indicated a positive correlation between soil colloidal P and colloidal iron, aluminum, and total organic carbon, suggesting that the mobilization of soil colloidal P could be facilitated through colloid dispersion processes. It should be noted that we did not directly measure the mass of soil colloids (< 1 µm) and thus did not determine the exact extent of colloid dispersion. Our data suggest that the calculated mass of soil aggregates < 2 µm tended to decrease with biochar addition, but this reduction was relatively minor compared to the 20–53 µm and 2–20 µm aggregate sizes (Fig. 2).

Our findings emphasize the importance of considering soil sorption properties when investigating the dynamics of soil colloidal P and dissolved P in response to biochar addition. In this context, it is crucial to evaluate the soil properties associated with P sorption, as these properties can also be influenced by biochar addition (Zhai et al. 2015; Zheng et al. 2020). Furthermore, it is important to note that our soil incubation experiment was conducted under controlled conditions with elevated biochar addition rates. Therefore, the results from our study should be validated at the field scale, particularly under long-term biochar incorporation conditions. This validation is particularly important as field-scale application could lead to significant biochar accumulation in the soil over time, similar to the high levels of biochar addition examined in our research.

5 Conclusion

Our study found that both rape straw-derived biochar and chicken manure-derived biochar positively influenced soil aggregation, primarily at the expense of soil aggregates within the 20–53 µm, 2–20 µm, and < 2 µm size classes. Chicken manure-derived biochar significantly increased soil P content, promoting a higher proportion of P allocation in soil aggregates of 53–250 µm and > 250 µm. In contrast, rape straw-derived biochar had a less pronounced impact on soil P dynamics.

Despite enhancing soil aggregate stability, chicken manure-derived biochar increased soil colloidal P and dissolved P. The elevated degree of P saturation resulting from chicken manure-derived biochar addition appeared to play a more crucial role in controlling soil colloidal P release and mobilization. Further investigation at the field scale is needed, especially for long-term biochar applications, to further understand how biochar amends affect soil colloidal P dynamics.

Supplementary Information The online version contains supplementary material available at https://doi.org/10.1007/s11368-024-03821-x.

Author contributions Jinju Wei: Formal analysis; Writing–original draft. Guobing Qin: Formal analysis. Qingyang Zeng: Formal analysis. Qi Luo: Formal analysis. Jianhua Ji: Funding acquisition; Writing–review and editing. Xiao Yan: Funding acquisition; Writing–review and editing. Jianfu Wu: Writing–review and editing. Zongqiang Wei: Conceptualization; Funding acquisition; Writing–original draft; Writing–review and editing.

Funding This work was supported by the National Natural Science Foundation of China (Nos. 41867019, 41967014, 32160754) and Natural Science Foundation of Jiangxi Province, China (No. 20212BAB205012).

Declarations

Competing interest The authors declare that there is no conflict of interest.

References

Biederman LA, Harpole WS (2013) Biochar and its effects on plant productivity and nutrient cycling: a meta–analysis. GCB Bioenergy 5:202–214. https://doi.org/10.1111/gcbb.12037

Blanco-Canqui H (2017) Biochar and soil physical properties. Soil Sci Soc Am J 81:687–711. https://doi.org/10.2136/sssaj2017.01.0017

Cao D, Lan Y, Sun Q, Yang X, Chen W, Meng J, Wang D, Li N (2021) Maize straw and its biochar affect phosphorus distribution in soil aggregates and are beneficial for improving phosphorus availability along the soil profile. Eur J Soil Sci 72:2165–2179. https://doi.org/10.1111/ejss.13095

Courchesne F, Turmel MC (2008) Extractable Al, Fe, Mn, and Si. In: Carter MR, Gregorich EG (eds) Soil Sampling and Methods of Analysis, 2nd edn. CRC Press, Taylor & Francis, Boca Raton, FL, pp 307–316

de Mendiburu F (2014) Agricolae: statistical procedures for agricultural research. R package version 1.1-8. https://cran.r-project.org/src/contrib/Archive/agricolae/

Dou Z, Ramberg CF, Toth JD, Wang Y, Sharpley AN, Boyd SE, Chen CR, Williams D, Xu ZH (2009) Phosphorus speciation and sorption-desorption characteristics in heavily manured soils. Soil Sci Soc Am J 73:93–101. https://doi.org/10.2136/sssaj2007.0416

Du Z, Zhao J, Wang Y, Zhang Q (2017) Biochar addition drives soil aggregation and carbon sequestration in aggregate fractions from an intensive agricultural system. J Soil Sediment 17:581–589. https://doi.org/10.1007/s11368-015-1349-2

Fresne M, Jordan P, Fenton O, Mellander P-E, Daly K (2021) Soil chemical and fertilizer influences on soluble and medium-sized colloidal phosphorus in agricultural soils. Sci Total Environ 754:142112. https://doi.org/10.1016/j.scitotenv.2020.142112

Garland G, Bünemann EK, Oberson A, Frossard E, Snapp S, Chikowo R, Six J (2018) Phosphorus cycling within soil aggregate fractions of a highly weathered tropical soil: A conceptual model. Soil Biol Biochem 116:91–98. https://doi.org/10.1016/j.soilbio.2017.10.007

Gu S, Gruau G, Dupas R, Jeanneau L (2020) Evidence of colloids as important phosphorus carriers in natural soil and stream waters in an agricultural catchment. J Environ Qual 49:921–932. https://doi.org/10.1002/jeq2.20090

Hosseini SH, Liang X, Niyungeko C, Miaomiao H, Li F, Khan S, Eltohamy KM (2019) Effect of sheep manure-derived biochar on colloidal phosphorus release in soils from various land uses. Environ Sci Pollut Res 26:36367–36379. https://doi.org/10.1007/s11356-019-06762-y

Ilg K, Siemens J, Kaupenjohann M (2005) Colloidal and dissolved phosphorus in sandy soils as affected by phosphorus saturation. J Environ Qual 34:926. https://doi.org/10.2134/jeq2004.0101

Islam MU, Jiang F, Guo Z, Peng X (2021) Does biochar application improve soil aggregation? A meta-analysis. Soil Till Res 209:104926. https://doi.org/10.1016/j.still.2020.104926

Jiang X, Bol R, Nischwitz V, Siebers N, Willbold S, Vereecken H, Amelung W, Klumpp E (2015a) Phosphorus containing water dispersible nanoparticles in arable soil. J Environ Qual 44:1772–1781. https://doi.org/10.2134/jeq2015.02.0085

Jiang X, Bol R, Willbold S, Vereecken H, Klumpp E (2015b) Speciation and distribution of P associated with Fe and Al oxides in aggregate-sized fraction of an arable soil. Biogeosciences 12:6443–6452. https://doi.org/10.5194/bg-12-6443-2015

Jin Y, Liang X, He M, Liu Y, Tian G, Shi J (2016) Manure biochar influence upon soil properties, phosphorus distribution and phosphatase activities: A microcosm incubation study. Chemosphere 142:128–135. https://doi.org/10.1016/j.chemosphere.2015.07.015

Jing Z, Chen R, Wei S, Lin X (2017) Biochar functions as phosphorous fertilizers in an alkaline alluvial soil. Commun Soil Sci Plant Anal 48:2455–2463. https://doi.org/10.1080/00103624.2017.1414830

Khan S, Liu C, Milham PJ, Eltohamy KM, Hamid Y, Jin J, He M, Liang X (2022) Nano and micro manure amendments decrease degree of phosphorus saturation and colloidal phosphorus release from agriculture soils. Sci Total Environ 845:157278. https://doi.org/10.1016/j.scitotenv.2022.157278

Kögel-Knabner I, Amelung W, Cao Z, Fiedler S, Frenzel P, Jahn R, Kalbitz K, Kölbl A, Schloter M (2010) Biogeochemistry of paddy soils. Geoderma 157:1–14. https://doi.org/10.1016/j.geoderma.2010.03.009

Kretzschmar R, Borkovec M, Grolimund D, Elimelech M (1999) Mobile subsurface colloids and their role in contaminant transport. In: Advances in Agronomy. Elsevier, pp 121–193

Kroetsch D, Wang C (2008) Particle size distribution. In: Carter MR, Gregorich EG (eds) Soil Sampling and Methods of Analysis, vol 2. CRC Press, pp 713–725

Kumari K, Moldrup P, Paradelo M, Elsgaard L, Hauggaard-Nielsen H, de Jonge LW (2014) Effects of biochar on air and water permeability and colloid and phosphorus leaching in soils from a natural calcium carbonate gradient. J Environ Qual 43:647–657. https://doi.org/10.2134/jeq2013.08.0334

Kuo S (1996) Phosphorus. In: Sparks DL (ed) Methods of soil analysis: Chemical methods Part 3 SSSA No.5. ASA-CSSA-SSSA. Madison, WI, pp 869–919

Li Q, Jin Z, Chen X, Jing Y, Huang Q, Zhang J (2017) Effects of biochar on aggregate characteristics of upland red soil in subtropical China. Environ Earth Sci 76:372. https://doi.org/10.1007/s12665-017-6703-9

Liang X, Jin Y, Zhao Y, Wang Z, Yin R, Tian G (2016) Release and migration of colloidal phosphorus from a typical agricultural field under long-term phosphorus fertilization in southeastern China. J Soil Sediment 16:842–853. https://doi.org/10.1007/s11368-015-1290-4

Liu Y, Ge T, Zhu Z, Liu S, Luo Y, Li Y, Wang P, Gavrichkova O, Xu X, Wang J, Wu J, Guggenberger G, Kuzyakov Y (2019) Carbon input and allocation by rice into paddy soils: A review. Soil Biol Biochem 133:97–107. https://doi.org/10.1016/j.soilbio.2019.02.019

Lu S, Sun F, Zong Y (2014) Effect of rice husk biochar and coal fly ash on some physical properties of expansive clayey soil (Vertisol). Catena 114:37–44. https://doi.org/10.1016/j.catena.2013.10.014

Murphy J, Riley J (1962) A modified single solution method for the determination of phosphate in natural waters. Anal Chim Acta 27:31–36. https://doi.org/10.1016/S0003-2670(00)88444-5

Ohno T, Zibilske LM (1991) Determination of low concentrations of phosphorus in soil extracts using malachite green. Soil Sci Soc Am J 55:892–895. https://doi.org/10.2136/sssaj1991.03615995005500030046x

Pituello C, Dal Ferro N, Francioso O, Simonetti G, Berti A, Piccoli I, Pisi A, Morari F (2018) Effects of biochar on the dynamics of aggregate stability in clay and sandy loam soils: Biochar effects on aggregate stability dynamics. Eur J Soil Sci 69:827–842. https://doi.org/10.1111/ejss.12676

Qin G, Yan X, Wei J, Wu J, Wei Z (2022) Does the carbon skeleton of biochar contribute to soil phosphate sorption? A case study from paddy soils with woody biochar amendment. Soil Res 60:242–251. https://doi.org/10.1071/SR21103

R Core Team (2019) R: A language and environment for statistical computing. Vienna, Austria: R Foundation for Statistical Computing. https://www.R-project.org/

Regelink IC, Koopmans GF, van der Salm C, Weng L, van Riemsdijk WH (2013) Characterization of colloidal phosphorus species in drainage waters from a clay soil using asymmetric flow field-flow fractionation. J Environ Qual 42:464–473. https://doi.org/10.2134/jeq2012.0322

Sachdeva V, Hussain N, Husk BR, Whalen JK (2019) Biochar-induced soil stability influences phosphorus retention in a temperate agricultural soil. Geoderma 351:71–75. https://doi.org/10.1016/j.geoderma.2019.05.029

Schmidt H, Kammann C, Hagemann N, Leifeld J, Bucheli TD, Sánchez Monedero MA, Cayuela ML (2021) Biochar in agriculture – A systematic review of 26 global meta-analyses. GCB Bioenergy 13:1708–1730. https://doi.org/10.1111/gcbb.12889

Siemens J, Ilg K, Lang F, Kaupenjohann M (2004) Adsorption controls mobilization of colloids and leaching of dissolved phosphorus. Eur J Soil Sci 55:253–263. https://doi.org/10.1046/j.1365-2389.2004.00596.x

Situ G, Zhao Y, Zhang L, Yang X, Chen D, Li S, Wu Q, Xu Q, Chen J, Qin H (2022) Linking the chemical nature of soil organic carbon and biological binding agent in aggregates to soil aggregate stability following biochar amendment in a rice paddy. Sci Total Environ 847:157460. https://doi.org/10.1016/j.scitotenv.2022.157460

Soinne H, Hovi J, Tammeorg P, Turtola E (2014) Effect of biochar on phosphorus sorption and clay soil aggregate stability. Geoderma 219:162–167. https://doi.org/10.1016/j.geoderma.2013.12.022

Sun F, Lu S (2014) Biochars improve aggregate stability, water retention, and pore- space properties of clayey soil. J Plant Nutr Soil Sci 177:26–33. https://doi.org/10.1002/jpln.201200639

Sun Q, Meng J, Lan Y, Shi G, Yang X, Cao D, Chen W, Han X (2021) Long-term effects of biochar amendment on soil aggregate stability and biological binding agents in brown earth. Catena 205:105460. https://doi.org/10.1016/j.catena.2021.105460

Turner BL, Mahieu N, Condron LM (2003) Phosphorus-31 nuclear magnetic resonance spectral assignments of phosphorus compounds in soil NaOH-EDTA extracts. Soil Sci Soc Am J 67:497–510. https://doi.org/10.2136/sssaj2003.4970

Usman ARA, Al-Wabel MI, Ok YS, Al-Harbi A, Wahb-Allah M, El-Naggar AH, Ahmad M, Al-Faraj A, Al-Omran A (2016) Conocarpus biochar induces changes in soil nutrient availability and tomato growth under saline irrigation. Pedosphere 26:27–38. https://doi.org/10.1016/S1002-0160(15)60019-4

Wang Y, Lin Y, Chiu PC, Imhoff PT, Guo M (2015) Phosphorus release behaviors of poultry litter biochar as a soil amendment. Sci Total Environ 512–513:454–463. https://doi.org/10.1016/j.scitotenv.2015.01.093

Wang S, Li T, Zheng Z (2016) Effect of tea plantation age on the distribution of soil organic carbon and nutrient within microaggregates in the hilly region of western Sichuan, China. Ecol Eng 90:113–119. https://doi.org/10.1016/j.ecoleng.2016.01.046

Wang Z, Chen L, Liu C, Jin Y, Li F, Khan S, Liang X (2021) Reduced colloidal phosphorus loss potential and enhanced phosphorus availability by manure-derived biochar addition to paddy soils. Geoderma 402:115348. https://doi.org/10.1016/j.geoderma.2021.115348

Xu G, Zhang Y, Shao H, Sun J (2016) Pyrolysis temperature affects phosphorus transformation in biochar: Chemical fractionation and 31P NMR analysis. Sci Total Environ 569–570:65–72. https://doi.org/10.1016/j.scitotenv.2016.06.081

Yan X, Wang D, Zhang H, Zhang G, Wei Z (2013) Organic amendments affect phosphorus sorption characteristics in a paddy soil. Agr Ecosyst Environ 175:47–53. https://doi.org/10.1016/j.agee.2013.05.009

Yan X, Wei Z, Hong Q, Lu Z, Wu J (2017) Phosphorus fractions and sorption characteristics in a subtropical paddy soil as influenced by fertilizer sources. Geoderma 295:80–85. https://doi.org/10.1016/j.geoderma.2017.02.012

Zhai L, CaiJi Z, Liu J, Wang H, Ren T, Gai X, Xi B, Liu H (2015) Short-term effects of maize residue biochar on phosphorus availability in two soils with different phosphorus sorption capacities. Biol Fert Soils 51:113–122. https://doi.org/10.1007/s00374-014-0954-3

Zheng H, Wang X, Luo X, Wang Z, Xing B (2018) Biochar-induced negative carbon mineralization priming effects in a coastal wetland soil: Roles of soil aggregation and microbial modulation. Sci Total Environ 610–611:951–960. https://doi.org/10.1016/j.scitotenv.2017.08.166

Zheng X, Wu J, Yan X, Qin G, Zhou R, Wei Z (2020) Biochar-induced soil phosphate sorption and availability depend on soil properties: a microcosm study. J Soil Sediment 20:3846–3856. https://doi.org/10.1007/s11368-020-02713-0